

Geophysical Research Letters[®]

RESEARCH LETTER

10.1029/2024GL111769

Key Points:

- Atlantic-Arctic cyclones exhibit large variability in thermodynamic characteristics, especially those of origin poleward of 70° N
- Large-scale atmospheric flow steers midlatitude-origin cyclones into the greater Barents region or preconditions the local environment
- “Warm” versus “cold” Arctic cyclones show differences in preconditioning and geographic clustering suggesting distinct genesis mechanisms

Supporting Information:

Supporting Information may be found in the online version of this article.

Correspondence to:

D. Tao,
ddantao@gmail.com

Citation:

Tao, D., Li, C., Davy, R., He, S., Spengler, T., Michel, C., & Rosendahl, A. (2025). Arctic-Atlantic cyclones: Variability in thermodynamic characteristics, large-scale flow, and local impacts. *Geophysical Research Letters*, 52, e2024GL111769. <https://doi.org/10.1029/2024GL111769>

Received 6 AUG 2024

Accepted 17 DEC 2024

Author Contributions:

Conceptualization: Dandan Tao, Camille Li, Richard Davy, Shengping He, Thomas Spengler

Formal analysis: Dandan Tao

Investigation: Dandan Tao

Methodology: Dandan Tao, Camille Li,

Richard Davy, Shengping He,

Thomas Spengler, Clio Michel

Supervision: Camille Li, Richard Davy

Validation: Dandan Tao,

Andrea Rosendahl

Visualization: Dandan Tao,

Andrea Rosendahl

Writing – original draft: Dandan Tao

Writing – review & editing: Dandan Tao,

Camille Li, Richard Davy, Shengping He,

Thomas Spengler, Clio Michel

© 2025. The Author(s).

This is an open access article under the terms of the [Creative Commons Attribution License](#), which permits use,

distribution and reproduction in any medium, provided the original work is properly cited.

Arctic-Atlantic Cyclones: Variability in Thermodynamic Characteristics, Large-Scale Flow, and Local Impacts

Dandan Tao^{1,2} , Camille Li^{1,2} , Richard Davy^{2,3} , Shengping He^{1,2}, Thomas Spengler^{1,2} , Clio Michel⁴ , and Andrea Rosendahl^{1,4}

¹Geophysical Institute, University of Bergen, Bergen, Norway, ²Bjerknes Centre for Climate Research, Bergen, Norway,

³Nansen Environmental and Remote Sensing Center, Bergen, Norway, ⁴Norwegian Meteorological Institute, Bergen, Norway

Abstract Cyclones at polar latitudes of the Atlantic-Arctic corridor exhibit different thermodynamic characteristics. Midlatitude-origin cyclones, which make up about 14% of wintertime cyclones in the region, are generally warm and moist. The more numerous Arctic-origin cyclones display a wide range in the boundary-layer equivalent potential temperature θ_e that depends on both temperature and moisture. This spread includes large positive and negative θ_e anomalies, leading to weak signals in composite means. Warm/moist (high- θ_e) cyclones at polar latitudes are associated with tilted and central jet regimes, steering cyclones of midlatitude-origin into the Barents region or preconditioning the environment for Arctic genesis. Conversely, cold/dry (low- θ_e) Arctic-origin cyclones form under a jet stream positioned far south, characterized by frequent southern jet regimes. These new insights into the large variability of Barents cyclones have implications for our understanding of genesis mechanisms, cyclone development, and their effect on the climate of the polar regions.

Plain Language Summary Cyclones transport heat and moisture poleward. In polar regions, they can cause extreme events such as heavy precipitation, winter heat waves, sea ice melt, rain-on-snow events, wind storms and coastal flooding. This study focuses on cyclones that form locally at high Arctic latitudes, whose characteristics and dynamical development are less known than those of midlatitude cyclones that travel to high latitudes. Cyclones that originate in the Arctic make up more than half of the cyclones identified in the greater Barents Sea region. They vary more widely in temperature and moisture than cyclones of remote origin entering the region: some are colder and drier than the climatological environment, while others are nearly as warm and moist as the cyclones from the midlatitude. The cold/dry (Arctic-origin) and warm/moist (of midlatitude or Arctic origin) cyclones are linked to distinct atmospheric flow patterns and opposing near-surface impacts in the polar regions. Our results indicate the importance of recognizing the diversity across Arctic cyclones to better understand their role in determining the climate and variability of the polar regions.

1. Introduction

Cyclones are a main driver of heat and moisture transport into the Arctic (Dufour et al., 2016; Fearon et al., 2021; Papritz & Dunn-Sigouin, 2020; Sorteberg & Walsh, 2008) as well as the weather systems responsible for most of the precipitation at high latitudes (Hartmuth et al., 2022; Hawcroft et al., 2012; Pfahl & Wernli, 2012). The energy fluxes, clouds, and precipitation associated with cyclones contribute to surface warming (Isaksen et al., 2016; Madonna et al., 2020; Messori et al., 2018; Murto et al., 2022; Rinke et al., 2017), sea ice melt (Dörr et al., 2021; Graham et al., 2019; Valkonen et al., 2021; Woods & Caballero, 2016), and large changes in the surface energy balance (Boisvert et al., 2016). In fact, cyclones are often involved in extreme weather at high latitudes, such as the record warming of 2015/2016 that raised surface temperatures above the melting point in the middle of winter (Binder et al., 2017; Boisvert et al., 2016; Moore, 2016) and the rain-on-snow events that affect ecosystems and infrastructure on Svalbard (Wickström et al., 2020). The extent of these cyclone-related surface impacts in the Arctic can differ greatly from case to case. Whether the diversity of impacts is linked to the different cyclone types present in the Arctic merits exploration.

The Barents Sea and Fram Strait form the main corridor for cyclones traveling poleward from the North Atlantic to the Arctic. Madonna et al. (2020) report approximately 15 cyclones in this region every winter season, of which the 10%–15% originating in the midlatitude North Atlantic are associated with the strongest surface warming signals. The authors also show a higher occurrence of cyclones when the North Atlantic jet stream is “unblocked” (not affected by persistent high-pressure systems blocking the westerly flow), extending toward the Barents

region with a southwest-northeast orientation. Interestingly, more than half of the cyclones in the Barents region are found to originate at high Arctic latitudes (north of 70 °N), but seem to be associated with weak surface warming signals according to composite analyses (Madonna et al., 2020). Given the sheer number of cyclones originating in the Barents Sea with scattered genesis locations, it is natural to wonder what insights may be gained by probing deeper into the weak composite warming signals.

Cyclones are typically characterized by their intensity (e.g., central low pressure), but moisture content associated with cyclones is also very important for determining their surface impacts on Arctic climate. There is generally not much moisture in the Arctic compared to lower latitudes, however, the moisture variability related to these weather features is extremely high within the Arctic. Because moisture enhances downwelling longwave radiation at the surface, which promotes surface warming and sea ice melt during winter when there is little incoming solar radiation (Messori et al., 2018; Woods & Caballero, 2016), using moisture and temperature to describe the thermodynamic character of a cyclone offers a useful alternative to cyclone intensity in understanding the severity of its surface impacts.

In this study, we investigate the thermodynamic variability of cyclones within the greater Barents Sea region of the Atlantic-Arctic corridor during the winter months, and how this thermodynamic variability affects surface conditions in the Arctic. Section 2 describes the data and methodology, Section 3 shows the results of the analysis, and Section 4 presents concluding remarks.

2. Data and Methodology

2.1. Reanalysis Data

We use the fifth generation ECMWF reanalysis (ERA5, Hersbach et al., 2020) for the period from 1979 to 2020 with a temporal resolution of 3 hr, and regrid the data to 0.5 × 0.5° spacing. Mean sea level pressure is used to identify cyclone tracks (see Section 2.2). Temperature (T in K) and moisture (mixing ratio q_v in g kg⁻¹) from 1,000 hPa to 200 hPa with 50 hPa intervals are used to calculate the vertical profiles of equivalent potential temperature $\theta_e = T \left(\frac{P_0}{P} \right)^{\frac{r_d}{C_p}} RH^{-\frac{r_d q_v}{C_p}} \exp \left(\frac{L_v q_v}{C_p T} \right)$, where $P_0 = 1000$ hPa is the reference pressure, P is pressure in hPa, RH is relative humidity, $r_d = 287.058$ J kg⁻¹ K⁻¹ is the gas constant for dry air, $C_p = 1,003.5$ J kg⁻¹ K⁻¹ is the heat capacity at constant pressure of dry air, $r_v = 461.495$ J kg⁻¹ K⁻¹ is the gas constant for water vapor, and $L_v = 2,501,000$ J kg⁻¹ is the latent heat of vapourization. To investigate the large-scale circulation, zonal wind at 850 hPa (U_{850} in m s⁻¹) and geopotential at 500 hPa (Φ_{500} in m² s⁻²) are used. Finally, to investigate surface signatures, we use the 2 m reference height temperature (T_{2m} in K), total column water vapor (TCWV, kg m⁻²), snow fraction defined as the ratio between snow and total precipitation, sensible and latent heat fluxes combined into a turbulent heat flux term (THFLX in W m⁻²), and downwelling longwave radiation at the surface (DLR in W m⁻²). For all thermodynamic fields, we remove the seasonal cycle and any quadratic trend at each latitude from the monthly mean data following Madonna et al. (2020).

2.2. Cyclone Identification and Classification

We use the Melbourne University algorithm to detect maxima in the Laplacian of mean sea level pressure in space and track them in time (Murray & Simmonds, 1996a, 1996b). Following Madonna et al. (2020), we keep only tracks lasting more than 2 days with genesis during the winter months (December, January and February, hereafter, DJF). The duration criterion excludes most short-lived polar lows and polar mesocyclones (Michel et al., 2018; Smirnova et al., 2015). Next, we choose the tracks that pass through the study region, comprising the Barents Sea and parts of the Greenland and Norwegian Seas (see black box in the first row of Figure 1). This extends the Barents Sea region used in Madonna et al. (2020) to the east coast of Greenland to cover the main corridor for winter midlatitude cyclones entering the Arctic (Sorteberg & Walsh, 2008). Finally, we categorize the tracks into three groups based on their origin:

- MIDLAT: cyclones entering the study region along the Atlantic-Arctic corridor with genesis south of 60 °N (94 tracks; Figure 1a)
- SUBARC: cyclones entering the study region along the Atlantic-Arctic corridor with genesis between 60 °N – 70 °N (199 tracks; Figure 1b)
- ARCTIC: cyclones with genesis in the study region (378 tracks; Figure 1c)

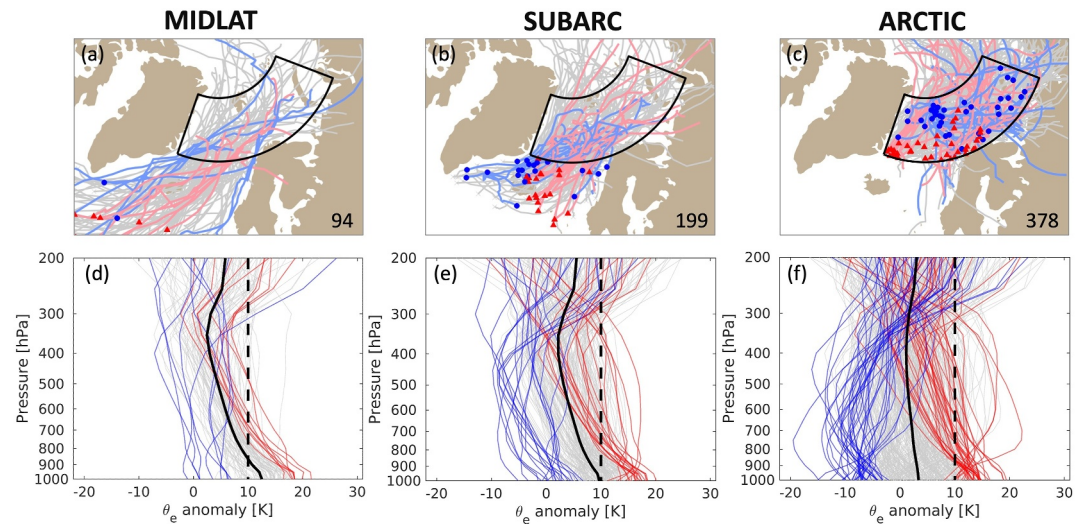


Figure 1. (a–c) Cyclone tracks for the three cyclone groups defined in Section 2.2: MIDLAT (left), SUBARC (center) and ARCTIC (right). The total number of tracks for each group is shown at the bottom right corner of each panel, and the study region is marked by the black box (70° – 80° N, 20° W– 70° E). The pink and light blue lines indicate the tracks for the high- θ_e and low- θ_e cyclones as defined by the 1,000–850 hPa equivalent potential temperature metric (see Section 2.2), respectively, and the filled red triangles and blue circles indicate the genesis locations (d–f) Vertical profiles of equivalent potential temperature (θ_e) anomalies averaged over a 500-km radius of the cyclone center at its first appearance in the study region relative to the equivalent potential temperature averaged over the study region for all DJF days. The red and blue lines indicate the high- θ_e and low- θ_e cyclones as defined by the 1,000–850 hPa equivalent potential temperature metric (see Section 2.2) and the gray lines are for all other cyclones. The thick black line is composite anomaly for each group, and the vertical dashed black line is a reference line for 10 K.

Given that cyclones carry heat and moisture poleward (Papritz & Dunn-Sigouin, 2020), we characterize them thermodynamically using θ_e . We define a metric of low-level (1,000–850 hPa) θ_e averaged over a 500-km radius from the surface low pressure center for each cyclone. For MIDLAT and SUBARC cyclones, this metric is calculated at the first time step when a cyclone enters the study region; for ARCTIC cyclones, it is calculated at the genesis time step. The top 10% in each group are designated as high- θ_e cyclones, and the bottom 10% as low- θ_e cyclones. The corresponding temperature and moisture anomaly profiles (Figure S1 in Supporting Information S1) show that, at low levels, the high- θ_e cyclones are both warm and moist while the low- θ_e cyclones are both cold and dry. There are 9, 20 and 38 cyclones in each of the high- θ_e and low- θ_e categories in the MIDLAT, SUBARC, and ARCTIC groups, respectively.

2.3. Large-Scale Atmospheric Circulation in Terms of Jet Regimes

We adopt the five North Atlantic jet regimes of Madonna et al. (2017) (their Figure 3) to study the relationship between high- θ_e /low- θ_e cyclones and the large-scale atmospheric circulation. The five regimes are tilted (T-jet), southern (S-jet), central (C-jet), northern (N-jet), and mixed (M-jet), with the names describing the location/orientation of the jet stream. Four of the five jet regimes are associated with the four main winter weather regimes identified in many studies (Michel & Rivière, 2011; Vautard, 1990). As shown in Madonna et al. (2017) and also in Figure S2 in Supporting Information S1, S-jet corresponds to Greenland Anticyclone, C-jet to Zonal, N-jet to Atlantic Ridge, M-jet to Scandinavian Blocking, while T-jet represents a combination of Zonal, Atlantic Ridge and Scandinavian blocking that projects on to a pattern known as European blocking. Each DJF day is assigned to one jet regime according to the highest pattern correlation between the daily U850 field and the mean U850 field associated with each regime (more details in Madonna et al., 2017). The climatological frequencies for winter jet regimes are 22% T-jet, 18% S-jet, 28% C-jet, 17% N-jet and 15% M-jet.

2.4. Bootstrap Significance Test

To assess the robustness of differences between high- θ_e and low- θ_e composites, we use a bootstrap resampling method that allows us to account for the different numbers of cyclones in each genesis group. We draw 1,000 samples of N cyclones with replacement (i.e., the same cyclone can be picked more than once), where $N = 9, 20$ and 38, respectively, for the MIDLAT, SUBARC and ARCTIC groups. Each sample thus contains the same number of cyclones as the composite for the group of interest, and the bootstrapped distribution of 1,000 samples gives a sense of how much variability is expected from random sampling. High- θ_e and low- θ_e composites falling far away from the median of the bootstrapped distribution (relative to the interquartile range) suggests that the differences between high- θ_e and low- θ_e cyclones are meaningful. The bootstrap results with replacement are nearly identical to a bootstrap test without replacement (not shown).

3. Results

3.1. Thermodynamic Characteristics of Cyclone Groups

Upon reaching the Arctic, cyclones of midlatitude origin are generally “warmer” (higher θ_e , meaning both higher temperature and more moisture) than cyclones of higher latitude origin. The average low-level θ_e of the MIDLAT cyclones as they enter the study area is about 12 K higher than the regional winter climatology, and the positive θ_e anomaly extends throughout the depth of the troposphere (black line in Figure 1d). The mean θ_e anomaly for the SUBARC group has a similar vertical structure to the MIDLAT group, but is weaker by approximately 2 K (Figure 1e). For the ARCTIC group, the θ_e anomaly profile is on average nearly the same as the study region's climatology but with a slightly warmer low levels (Figure 1f). From these average θ_e profiles, we find that cyclones of midlatitude origin are associated with a warmer low-level thermodynamic structure.

In addition to differences in the average θ_e between genesis groups, there are differences in the inter-group spread in θ_e , with ARCTIC cyclones exhibiting the largest variability. The maximum low-level θ_e anomaly is nearly equivalent across the three groups (~ 20 K), meaning that very warm, moist cyclones may originate anywhere within the Atlantic-Arctic corridor. The minimum boundary-layer θ_e anomaly ranges from around 0 K for MIDLAT and -5 K for SUBARC to -15 K for ARCTIC. With a range of 35 K between the maximum and minimum boundary-layer θ_e , the ARCTIC group has a spread nearly twice as large as that of the MIDLAT group. Moreover, the coldest/driest cyclones in the ARCTIC group are associated with colder, drier conditions than climatology (all days, including those when no cyclone is present), a rather surprising result as cyclones are expected to be associated with moistening and warming. We will come back to this in Section 3.2.

The corresponding temperature and moisture profiles (Figure S1 in Supporting Information S1) are consistent with the θ_e anomalies such that both temperature and moisture contribute to the differences observed in θ_e . The large θ_e spread across the ARCTIC group (Figure 1f) sheds light on the weak warming signal in the composite over all cyclones of high latitude origin shown by Madonna et al. (2020): it results from averaging over cyclones with strong but opposite-signed temperature/moisture anomalies that largely cancel each other out.

Note that the MIDLAT group has far fewer cyclones than the other two genesis groups, leading to less representative results. However, the MIDLAT cyclones also tend to be more similar to each other thermodynamically (small spread in Figure 1d) than the cyclones in the other groups. Together with the bootstrap tests, which account for different sample sizes, this lends confidence to the reported results.

3.2. Differences in Environmental Conditions Between High- θ_e and Low- θ_e Cyclones

The high- θ_e and low- θ_e cyclones show preferred entry or genesis locations in the study region. High- θ_e cyclones of MIDLAT and SUBARC origin tend to enter the region in the middle of the Norwegian Sea, while low- θ_e cyclones enter further west along the Greenland coast with a few along the coast of Norway (Figures 1a and 1b). For the ARCTIC group, the majority of high- θ_e cyclones form in the southwestern part of the study region over open ocean, while most of low- θ_e cyclones form in the northern and eastern parts of the study region near the climatological winter sea ice edge (Figure 1c). The geographic clustering suggests that there are differences in the environmental conditions associated with high- θ_e and low- θ_e cyclones.

High- θ_e cyclones consistently show warm anomalies in the Barents-Scandinavian region regardless of their origin, as seen in composites of 2-m temperature (Figure 2). For the MIDLAT and SUBARC groups, the warm

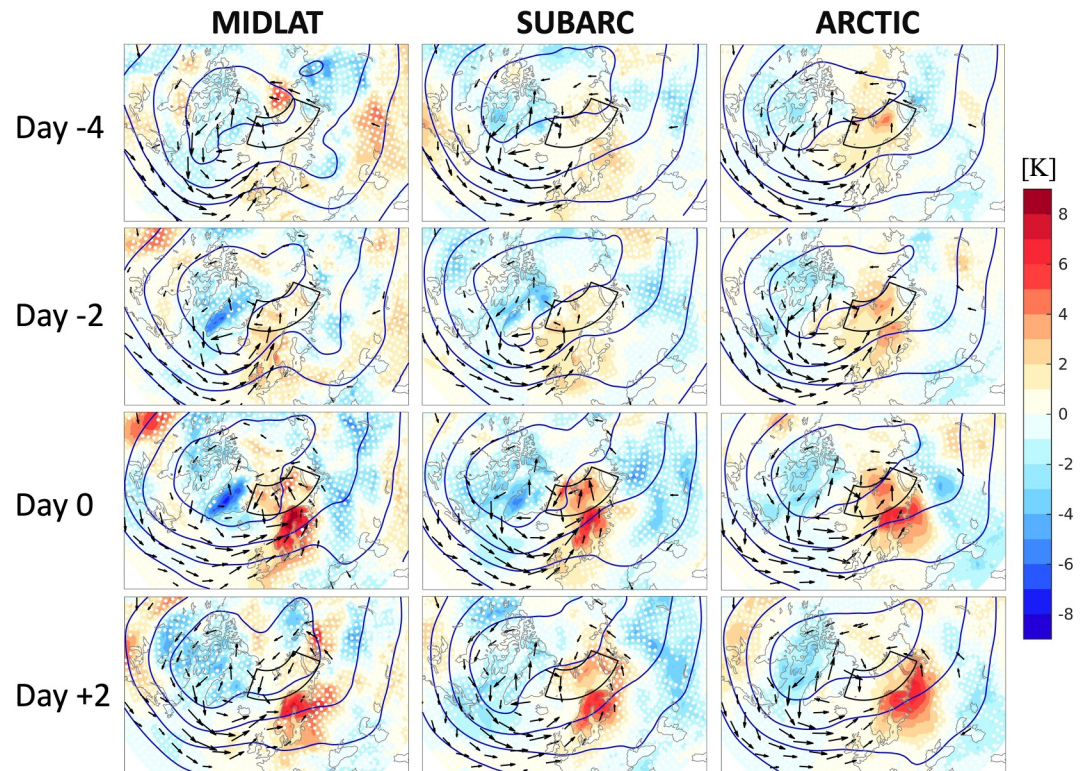


Figure 2. Large-scale conditions associated with high- θ_e cyclones in the MIDLAT (left), SUBARC (center) and ARCTIC (right) groups. Composites of detrended daily T2m anomalies (shading in K, white dots indicate regions not passing a two-sided t -test at a significance level of 0.05), daily 10-m wind (vectors, only for wind speed $> 3 \text{ m s}^{-1}$) and geopotential at 500 hPa (blue contours, $2 \times 10^4 \text{ m}^2 \text{ s}^{-2}$ interval) shown at time lags -4 , -2 , 0 and $+2$ days for high- θ_e cyclones in each group. Day 0 is defined as the day when the track enters the study region for the MIDLAT and SUBARC groups, and the genesis day for the ARCTIC group.

surface anomalies strengthen from Day -4 to Day 0 as the cyclones approach the study region from lower latitudes (Figure 2, left and middle columns), pushing warm and moist air ahead of their low-pressure centers. For the ARCTIC group, the anomalous warming signal prior to Day 0 indicates a warm and moist environment even before cyclogenesis (Figure 2 and S3 in Supporting Information S1, right column), and is further enhanced by the formation of the high- θ_e cyclone.

Low- θ_e cyclones show negative anomalies of temperature and moisture over large parts of the study region (Figure 3 and S4 in Supporting Information S1). This is somewhat unexpected, as cyclones are generally associated with the poleward transport of warm, moist air masses. For the MIDLAT and SUBARC groups, the cold anomalies weaken after the cyclones enter the study region, suggesting that the cyclones themselves do transport warm air, but into such a cold environment that the total temperature anomaly is negative.

For the ARCTIC group, the study region is dominated by cold anomalies throughout Day -4 to Day $+2$. The cold anomalies that exist prior to Day 0 means that low- θ_e ARCTIC cyclones form in a preconditioned cold and dry environment. Furthermore, the continuation of strong cold anomalies after Day 0 suggests that the formation and development of the low- θ_e ARCTIC cyclones have a limited effect on the environmental temperature and moisture. This is consistent with the θ_e profiles for the low- θ_e ARCTIC cyclones being much colder/drier than the regional climatology (Figure 1f).

3.3. Differences in Large-Scale Atmospheric Circulation Associated With High- θ_e and Low- θ_e Cyclones

The results in Section 3.2 suggest a role for large-scale atmospheric circulation patterns in setting up a range of different environmental conditions through advection of air masses and steering of cyclones. The high- θ_e cyclones are all—regardless of origin—associated with near-surface (10 m) southwesterly winds advecting warm

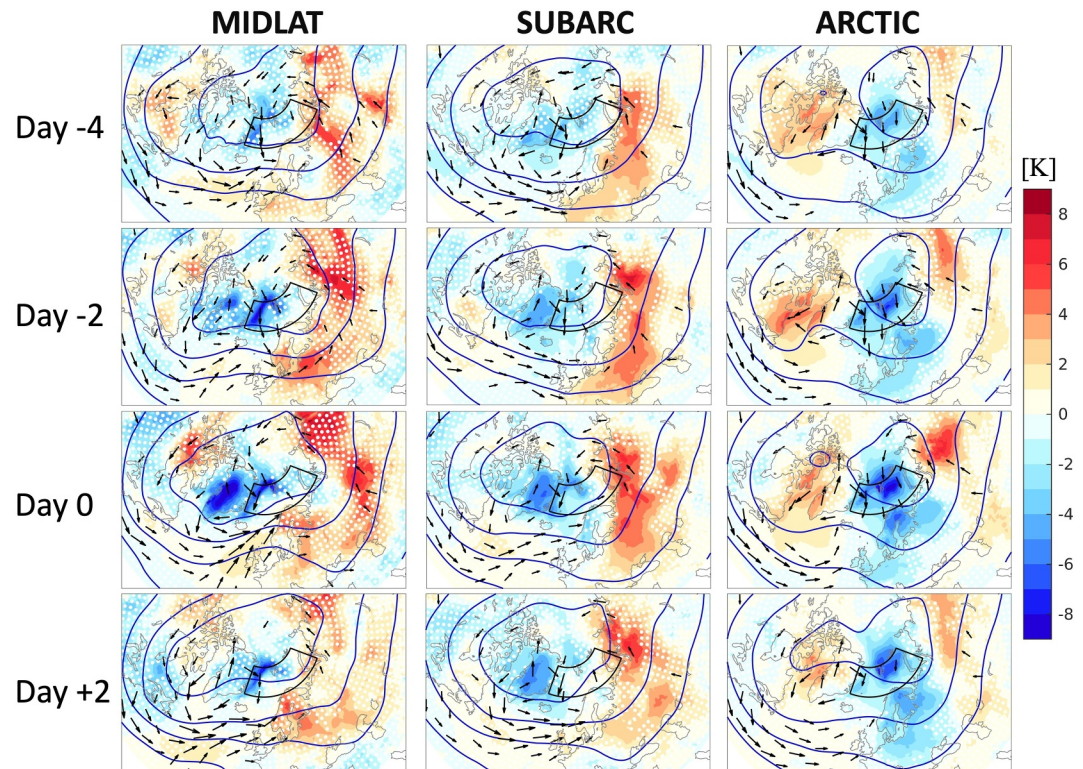


Figure 3. Same as Figure 2 but for low- θ_e cyclones.

air toward the study region (Figure 2, black arrows), consistent with an upstream trough in the $\Phi 500$ field that is present before Day 0 (blue contours). The low- θ_e cyclones in the MIDLAT group (Figure 3, left column) also show this circulation pattern but with weaker warm anomalies.

The low- θ_e composites from the SUBARC and ARCTIC groups are different, however, with wind coming from the north advecting cold air into the study region. The effect is more prominent for ARCTIC cyclones, and the strong northerly winds before Day 0 (Figure 3, right column) point to their role in preconditioning the great Barents region prior to cyclogenesis. The $\Phi 500$ field indicates a rather zonal orientation of the mid-tropospheric flow for SUBARC low- θ_e cyclones, and a clear ridge just upstream of the study region for ARCTIC low- θ_e cyclones.

The differences in circulation patterns for each genesis group are reflected in the jet stream. Further breaking down the mean jet anomalies into contributions from the jet regimes (see Section 2.3) allows us to better account for the large day-to-day variability in the jet position, orientation and extent (Figure S2 in Supporting Information S1). The cyclones in the MIDLAT group preferentially reach the study region when the jet exhibits a southwest-northeast orientation and an extension up toward Scandinavia (Figure 4a). We find that this arises from a high frequency of the tilted T-jet regime and a low frequency of the southern S-jet regime for all cyclones in the group (Figure 4d, gray bars). Medians of the bootstrapped jet distribution show 42% T-jet days and 4% S-jet days compared to the climatological winter values of 22% and 18% (black bars). The result holds for both high- θ_e (pink dots) and low- θ_e cyclones (blue dots), with a more pronounced discrepancy for the high- θ_e cyclones.

In contrast to the similarity of the jet stream across the MIDLAT group, the jet stream differs substantially for high- θ_e and low- θ_e cyclones in the ARCTIC group. The high- θ_e composite shows a more tilted and eastward-extended jet than the low- θ_e composite (Figure 4c), corresponding to striking differences in the jet regime distribution (Figure 4f). The southern S-jet and central C-jet frequencies with high- θ_e and low- θ_e cases lie on far opposite sides of the interquartile spread of the bootstrapped distribution. The tilted T-jet frequency differences are smaller, but still considerable, with the high- θ_e case lying well above the 75th percentile and the low- θ_e case at the 25th percentile. Overall, however, the bootstrapped distribution of jet frequencies for the ARCTIC group is

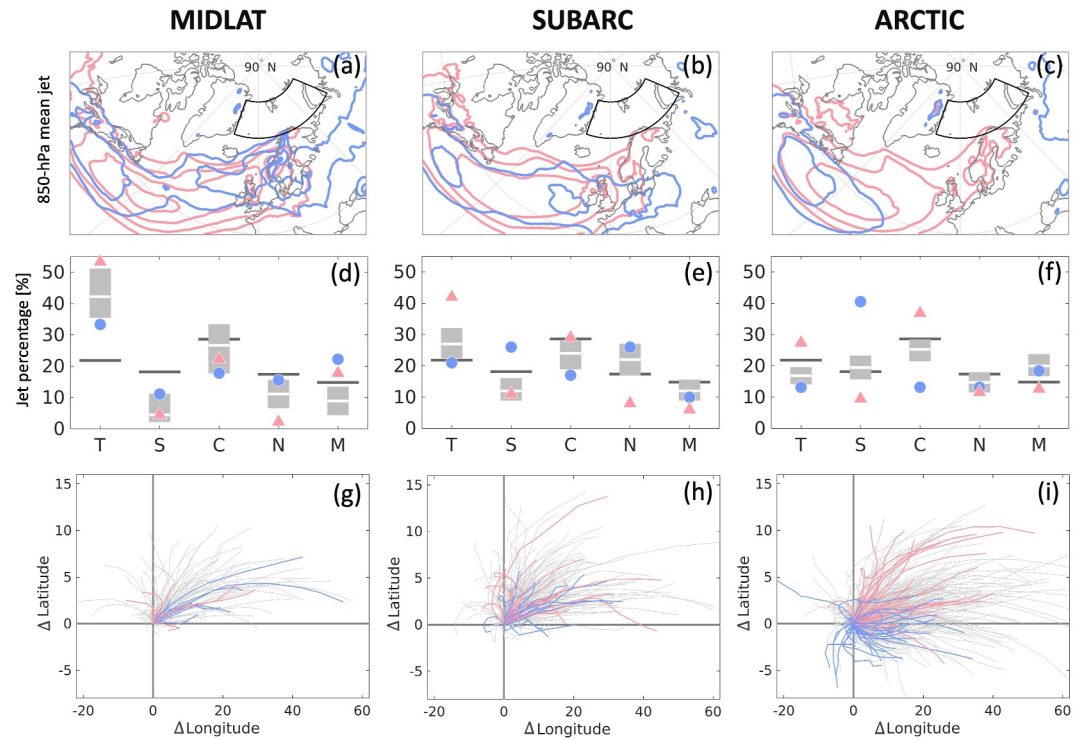


Figure 4. Jet stream and track directions associated with cyclones in the MIDLAT (left), SUBARC (center) and ARCTIC (right) groups (a–c) Composites of U850 averaged from Day –4 to Day 0 with contour intervals of 2.5 ms^{-1} starting from 7.5 ms^{-1} , pink for high- θ_e cyclones and blue for low- θ_e cyclones. Day 0 is the arrival day in study region for MIDLAT and SUBARC cyclones, and the genesis day for ARCTIC cyclones (d–f) Frequency of jet regimes from Day –4 to Day 0. The letters represent tilted (T), southern (S), central (C), northern (N) and mixed (M) jet regimes, as shown in Figure S2 in Supporting Information S1. Pink triangles are for high- θ_e cyclones and blue circles are for low- θ_e cyclones. The gray bars show the interquartile spread from a bootstrap significance test (see Section 2.4 for details), with the median indicated by the white bar. The horizontal black bar indicates the winter climatology of jet regime frequencies calculated from all DJF days of 1979–2020 (g–i) Direction of 24-hr cyclone tracks relative to the location of entry (MIDLAT and SUBARC) or genesis (ARCTIC) of the cyclone in the study region, with pink for high- θ_e cyclones, blue for low- θ_e cyclones and gray for all other cyclones in the group.

quite similar to climatology (Figure 4f, black bars). This result, together with the high- θ_e /low- θ_e differences, indicates that there is no preferred jet regime for genesis of ARCTIC cyclones, but that central and tilted jet days favor the formation of high- θ_e cyclones, while southern jet days favor the formation of low- θ_e cyclones.

The jet frequencies associated with SUBARC cyclones show mixed characteristics of both MIDLAT and ARCTIC groups. The high- θ_e cyclones have more tilted T-jet and central C-jet days and fewer southern S-jet days, similar to the regime distribution for MIDLAT high- θ_e cyclones. The distribution for low- θ_e cyclones is quite flat with only slightly higher percentages of southern S-jet and northern N-jet days.

The tracks of individual cyclones inside the study region also reflect the differences in jet regimes. In the ARCTIC group, the tracks for high- θ_e and low- θ_e cyclones show distinct directions: the majority of high- θ_e cyclones travel northeastward after genesis, consistent with the dominance of central C-jet and tilted T-jet regimes, whereas the majority of low- θ_e cyclones travel southeastward after genesis. No clear separation of tracks is found for high- θ_e and low- θ_e cyclones in the MIDLAT and SUBARC groups, as expected from the smaller contrast in the jet regime distributions between the high- θ_e and low- θ_e cyclones.

3.4. Surface Signatures

To clarify if the large spread in the thermodynamic characteristics (temperature, moisture) of cyclones within our study area translate into a large spread in other surface signatures, we analyze the winter surface energy budget. Specifically, we focus on downwelling longwave radiation, surface turbulent heat flux and the proportion of total precipitation falling as snow and look for differences between high- θ_e and low- θ_e cyclones (Figure 5).

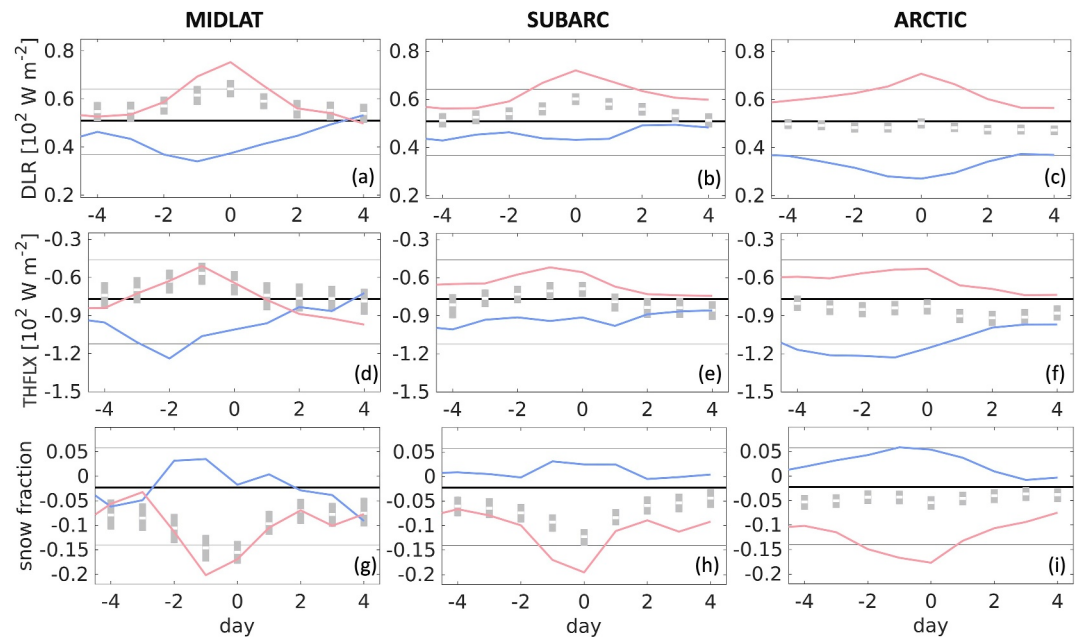


Figure 5. Surface energy budget and impacts associated with MIDLAT (left), SUBARC (center) and ARCTIC (right) cyclones (a–c) Downwelling longwave radiation (DLR) (d–f) surface turbulent heat flux (THFLX, negative indicates from surface to atmosphere), and (g–i) snow to total precipitation ratio (snow fraction) averaged within the study region. The gray bars show the interquartile spread from a bootstrap significance test (see Section 2.4 for details), with the median indicated by white horizontal bar. Pink lines show the time evolution for the high- θ_e cyclones, blue lines show the time evolution for the low- θ_e cyclones. The median and the 25th and 75th percentiles of all DJF daily mean values averaged within the study region are shown as the thick black horizontal line and the thin gray lines, respectively. All fields shown are detrended using monthly mean data at each latitude.

On average, the presence of MIDLAT and SUBARC cyclones moves surface conditions in the study region away from climatology, while the presence of ARCTIC cyclones does not. With the arrival of the MIDLAT and SUBARC cyclones (from Day 0), the medians of the three variables of interest (Figure 5, white horizontal bar) are anomalous relative to the daily climatological values for DJF (left and center columns), while the medians associated with the ARCTIC cyclones lie close to climatology (right column). Our assessment of the amount by which the medians deviate from climatology takes into account the sampling uncertainty, estimated via the interquartile spread from a bootstrap significance test (gray bars; see Section 2.4 for details). With the passage and decay of MIDLAT and SUBARC cyclones in the study region (after Day 2), all variables gradually become less anomalous, which means the surface conditions in the study region return to their climatological values.

In addition, surface conditions are significantly different between high- θ_e (Figure 5, pink lines) and low- θ_e cyclones (blue lines), regardless of genesis location. With higher air temperatures and more moisture in the high- θ_e cyclones, there is more downwelling longwave radiation (first row) and weaker (less negative) ocean-to-atmosphere turbulent heat flux (second row) on days when these are present compared to the days with low- θ_e cyclones. The warmer low-level air temperature in the high- θ_e cyclones also results in more precipitation falling as rain (third row), which indicates more potential for rain-on-snow events. For the high- θ_e and low- θ_e ARCTIC cyclones, the aforementioned preconditioning of the environment is again evident, with downwelling longwave and turbulent fluxes sitting well outside the interquartile range of all DJF days from 4 days before cyclogenesis.

4. Concluding Remarks

Cyclones reaching polar latitudes through the Atlantic-Arctic corridor are found to exhibit different thermodynamic characteristics as measured by low-level temperature and moisture. Cyclones of midlatitude origin are generally warm and moist, while those of Arctic origin can differ greatly from each other, with a spread in boundary-layer equivalent potential temperature nearly twice as large as that of the midlatitude cyclones. Not only is the spread larger, it spans opposite-signed anomalies in circulation patterns and environmental conditions

relative to climatology. Thus, cyclones with Arctic genesis may exhibit very different near-surface impacts despite their composite signal appearing weak (a result of averaging over large positive and negative anomalies).

While a southwest-northeast oriented jet stream is known to be linked to more cyclones in the Barents Sea (Madonna et al., 2020), our analysis offers additional insights. Generally, a low frequency of the southern jet regime together with a high frequency of the tilted or central jet regime are associated with warm/moist conditions in the Arctic, either via the steering of midlatitude-origin cyclones into the greater Barents region or via preconditioning the environment prior to the (local) formation of warm/moist cyclones (i.e., high- θ_e cyclones in the ARCTIC group). In contrast, cold/dry cyclones of Arctic origin (low- θ_e cyclones in the ARCTIC group) form under a different circulation pattern featuring a jet stream positioned far to the south, with a high frequency of the southern jet regime and a low frequency of the central jet regime.

The genesis locations for cyclones that form in the Arctic show geographic clustering, with high- θ_e genesis occurring mainly over open ocean and low- θ_e genesis occurring near the climatological winter sea ice edge. Along with the preconditioning mentioned previously, this suggests the possibility of distinct sources of baroclinicity and genesis mechanisms. The fact that high- θ_e cyclones form when the region is already warm and moist with tilted jets being prevalent points to the recent passage of a midlatitude cyclone (Priestley et al., 2020) or weather system (e.g., a cyclone off the southwest coast of Greenland, or blocking over Scandinavia) that favors moisture transport into the Arctic (Papritz & Dunn-Sigouin, 2020). The low- θ_e cyclones' affinity for the sea ice edge indicates that local, near-surface baroclinicity drives their genesis. Furthermore, visual inspection of individual genesis events suggests that interactions with co-occurring cyclones likely contribute to the picture. The differences between the development environments of high- θ_e and low- θ_e cyclones imply different genesis mechanisms. Future work will aim to disentangle these underexplored aspects of Arctic cyclogenesis and cyclone development.

Data Availability Statement

The ERA5 global reanalysis data set (Hersbach et al., 2020) is used in this study. Single-level data is available from Hersbach et al. (2023a) and pressure-level data is available from Hersbach et al. (2023b).

References

- Binder, H., Boettcher, M., Grams, C. M., Joos, H., Pfahl, S., & Wernli, H. (2017). Exceptional air mass transport and dynamical drivers of an extreme wintertime Arctic warm event. *Geophysical Research Letters*, *44*(23), 12028–12036. <https://doi.org/10.1002/2017GL075841>
- Boisvert, L. N., Petty, A. A., & Stroeve, J. C. (2016). The impact of the extreme winter 2015/16 Arctic cyclone on the Barents-Kara seas. *Monthly Weather Review*, *144*(11), 4279–4287. <https://doi.org/10.1175/MWR-D-16-0234.1>
- Dörr, J., Árhun, M., Eldevik, T., & Madonna, E. (2021). Mechanisms of regional winter sea-ice variability in a warming Arctic. *Journal of Climate*, *34*(21), 8635–8653. <https://doi.org/10.1175/JCLI-D-21-0149.1>
- Dufour, A., Zolina, O., & Gulev, S. K. (2016). Atmospheric moisture transport to the Arctic: Assessment of reanalyses and analysis of transport components. *Journal of Climate*, *29*(14), 5061–5081. <https://doi.org/10.1175/JCLI-D-15-0559.1>
- Fearon, M. G., Doyle, J. D., Ryglicki, D. R., Finocchio, P. M., & Sprenger, M. (2021). The role of cyclones in moisture transport into the Arctic. *Geophysical Research Letters*, *48*(4), e2020GL090353. <https://doi.org/10.1029/2020GL090353>
- Graham, R. M., Itkin, P., Meyer, A., Sundfjord, A., Spreen, G., Smedsrud, L. H., et al. (2019). Winter storms accelerate the demise of sea ice in the Atlantic sector of the Arctic Ocean. *Scientific Reports*, *9*(1), 9222. <https://doi.org/10.1038/s41598-019-45574-5>
- Hartmuth, K., Boettcher, M., Wernli, H., & Papritz, L. (2022). Identification, characteristics and dynamics of Arctic extreme seasons. *Weather and Climate Dynamics*, *3*(1), 89–111. <https://doi.org/10.5194/wcd-3-89-2022>
- Hawcroft, M. K., Shaffrey, L. C., Hodges, K. I., & Dacre, H. F. (2012). How much Northern Hemisphere precipitation is associated with extratropical cyclones? *Geophysical Research Letters*, *39*(24), L24809. <https://doi.org/10.1029/2012GL053866>
- Hersbach, H., Bell, B., Berrisford, P., Biavati, G., Horányi, A., Muñoz-Sabater, J., et al. (2023a). ERA5 hourly data on single levels from 1940 to present. *Copernicus Climate Change Service (C3S) Climate Data Store (CDS)*. [Dataset]. <https://doi.org/10.24381/cds.adbb2d47>
- Hersbach, H., Bell, B., Berrisford, P., Biavati, G., Horányi, A., Muñoz-Sabater, J., et al. (2023b). ERA5 hourly data on pressure levels from 1940 to present. *Copernicus Climate Change Service (C3S) Climate Data Store (CDS)*. [Dataset]. <https://doi.org/10.24381/cds.bd0915c6>
- Hersbach, H., Bell, B., Berrisford, P., Hirahara, S., Horányi, A., Muñoz-Sabater, J., et al. (2020). The ERA5 global reanalysis. *Quarterly Journal of the Royal Meteorological Society*, *146*(730), 1999–2049. <https://doi.org/10.1002/qj.3803>
- Isaksen, K., Nordli, Ø., Førland, E. J., Lupikasza, E., Eastwood, S., & Niedźwiedź, T. (2016). Recent warming on Spitsbergen—Influence of atmospheric circulation and sea ice cover. *Journal of Geophysical Research: Atmospheres*, *121*, 11913–11931. <https://doi.org/10.1002/2016JD025606>
- Madonna, E., Hes, G., Li, C., Michel, C., & Siew, P. Y. F. (2020). Control of Barents Sea wintertime cyclone variability by large-scale atmospheric flow. *Geophysical Research Letters*, *47*(19), e2020GL090322. <https://doi.org/10.1029/2020GL090322>
- Madonna, E., Li, C., Grams, C. M., & Woollings, T. (2017). The link between eddy-driven jet variability and weather regimes in the North Atlantic-European sector. *Quarterly Journal of the Royal Meteorological Society*, *143*(708), 2960–2972. <https://doi.org/10.1002/qj.3155>
- Messori, G., Woods, C., & Caballero, R. (2018). On the drivers of wintertime temperature extremes in the high Arctic. *Journal of Climate*, *31*(4), 1597–1618. <https://doi.org/10.1175/JCLI-D-17-0386.1>

Acknowledgments

This work was supported by funding from the Research Council of Norway (Grants 276730, 328938 and 325440) and Utdannings-og forskningsdepartementet (Fast-track-initiative from Bjerknes Centre for Climate Research).

- Michel, C., & Rivière, G. (2011). The link between rossby wave breakings and weather regime transitions. *Journal of the Atmospheric Sciences*, 68(8), 1730–1748. <https://doi.org/10.1175/2011JAS3635.1>
- Michel, C., Terpstra, A., & Spengler, T. (2018). Polar mesoscale cyclone climatology for the Nordic Seas based on ERA-Interim. *Journal of Climate*, 31(6), 2511–2532. <https://doi.org/10.1175/JCLI-D-16-0890.1>
- Moore, G. W. K. (2016). The December 2015 North Pole warming event and the increasing occurrence of such events. *Scientific Reports*, 6(1), 39084. <https://doi.org/10.1038/srep39084>
- Murray, R. J., & Simmonds, I. (1996a). A numerical scheme for tracking cyclone centres from digital data. Part I: Development and operation of the scheme. *Australian Meteorological Magazine*, 39, 155–166.
- Murray, R. J., & Simmonds, I. (1996b). A numerical scheme for tracking cyclone centres from digital data. Part II: Application to January and July general circulation model simulations. *Australian Meteorological Magazine*, 39, 167–180.
- Murto, S., Caballero, R., Svensson, G., & Papritz, L. (2022). Interaction between Atlantic cyclones and Eurasian atmospheric blocking drives wintertime warm extremes in the high Arctic. *Weather and Climate Dynamics*, 3(1), 21–44. <https://doi.org/10.5194/wcd-3-21-2022>
- Papritz, L., & Dunn-Sigouin, E. (2020). What configuration of the atmospheric circulation drives extreme net and total moisture transport into the Arctic. *Geophysical Research Letters*, 47(17), e2020GL089769. <https://doi.org/10.1029/2020GL089769>
- Pfahl, S., & Wernli, H. (2012). Quantifying the relevance of cyclones for precipitation extremes. *Journal of Climate*, 25(19), 6770–6780. <https://doi.org/10.1175/JCLI-D-11-00705.1>
- Priestley, M. D. K., Dacre, H. F., Shaffrey, L. C., Schemm, S., & Pinto, J. G. (2020). The role of secondary cyclones and cyclone families for the North Atlantic storm track and clustering over western Europe. *Quarterly Journal of the Royal Meteorological Society*, 146(728), 1184–1205. <https://doi.org/10.1002/qj.3733>
- Rinke, A., Maturilli, M., Graham, R. M., Matthes, H., Handorf, D., Cohen, L., et al. (2017). Extreme cyclone events in the Arctic: Wintertime variability and trends. *Environmental Research Letters*, 12(9), 094006. <https://doi.org/10.1088/1748-9326/aa7def>
- Smirnova, J. E., Golubkin, P. A., Bobylev, L. P., Zabolotskikh, E. V., & Chapron, B. (2015). Polar low climatology over the Nordic and Barents seas based on satellite passive microwave data. *Geophysical Research Letters*, 42(13), 5603–5609. <https://doi.org/10.1002/2015GL063865>
- Sorteberg, A., & Walsh, J. E. (2008). Seasonal cyclone variability at 70°N and its impact on moisture transport into the Arctic. *Tellus*, 60(3), 570–586. <https://doi.org/10.1111/j.1600-0870.2008.00314.x>
- Valkonen, E., Cassano, J., & Cassano, E. (2021). Arctic cyclones and their interactions with the declining sea ice: A recent climatology. *Journal of Geophysical Research: Atmospheres*, 126(12), e2020JD034366. <https://doi.org/10.1029/2020JD034366>
- Vautard, R. (1990). Multiple weather regimes over the north atlantic: Analysis of precursors and successors. *Monthly Weather Review*, 118(10), 2056–2081. [https://doi.org/10.1175/1520-0493\(1990\)118<2056:MWROTN>2.0.CO;2](https://doi.org/10.1175/1520-0493(1990)118<2056:MWROTN>2.0.CO;2)
- Wickström, S., Jonassen, M. O., Cassano, J. J., & Vihma, T. (2020). Present temperature, precipitation, and rain-on-snow climate in Svalbard. *Journal of Geophysical Research: Atmospheres*, 125(14), e2019JD032155. <https://doi.org/10.1029/2019JD032155>
- Woods, C., & Caballero, R. (2016). The role of moist intrusions in winter Arctic warming and sea ice decline. *Journal of Climate*, 29(12), 4473–4485. <https://doi.org/10.1175/JCLI-D-15-0773.1>